Measurement 158 (2020) 107750

Contents lists available at ScienceDirect

Measurement

journal homepage: www.elsevier.com/locate/measurement

Surface flatness and roughness evolution after magnetic assisted ball burnishing of magnetizable and non-magnetizable materials

Zsolt F. Kovács [a,c], Zsolt J. Viharos [a,b,*], János Kodácsy [a]

[a] John von Neumann University, GAMF Faculty of Engineering and Computer Science, Dep. of Vehicle and Faculty of Economics and Business, Dep. of Economics and Law, Kecskemét H-6000, Hungary
[b] Institute for Computer Science and Control, Research Laboratory on Engineering and Management Intelligence, Budapest H-1111, Hungary
[c] Budapest University of Technology and Economics, Department of Manufacturing Science and Technology, Budapest H-1111, Hungary

ARTICLE INFO

Article history:
Received 14 November 2019
Received in revised form 18 January 2020
Accepted 11 March 2020
Available online 18 March 2020

Keywords:
Magnetic
Ball burnishing
Surface roughness
Taguchi
Material hardness
Flatness
Fine grain

ABSTRACT

The burnishing process is applied to improve the surface roughness and hardness. The goal of the reported research was to evaluate the machining conditions on magnetisable and non-magnetisable materials by the novel permanent magnetic assisted ball burnishing (MABB) tool. The MABB tool was designed to reduce the surface roughness but this process has further effects on the surface C45 steel, X6CrNiTi1811 austenite steel, AA7075 aluminium alloy and PA6 polymer materials were burnished in the experiments. Surface quality is a complex feature that refers to the micro-geometrical characteristics of the machined surface. It includes roughness and waviness and gives a realistic picture about the top layer of the surface, while micro hardness and grains structure are especially important on sub-surface level. Results according to these analysed aspects mirrored that all of the tested materials can be burnished by the novel MABB tool, however, the effects from the economical viewpoints are diverse.

1. Introduction

The magnetic assisted ball burnishing (MABB) process is one of the cold-plastic finishing processes. It differs from other finishing solutions, such as hand scraping, lapping, grinding [1,2] etc., because it decreases the residual tension stresses on the machined surface (Fig. 1) [3].

Furthermore, MABB is economically beneficial, because it is a simple and cheap process that requires short time and easy preparations. The introduced MABB process is unique, because the conventional burnishing is applied for finishing internal or external cylindrical surfaces, while the introduced MABB tool is suitable for flat or harmonically flat surfaces. The designed tool is shown in Fig. 2 [4].

The presented tool can be applied in conventional and CNC-controlled machines, too. During the analysis the tool is continuously cooled internally by minimum quantity lubrication (MQL) oil. During this flat surface machining, while the tool moves on the planed path at the given feed rate, at the same time it rotates with a specific speed and as result it rolls down the surface. In case of ferromagnetic materials, the required burnishing force is provided by the attractiveness of the balls, if the tool approaches the workpiece at a given *h* distance [5] (Fig. 2). However, this magnetic force cannot be established on non-magnetizable materials, because the magnetic attraction between the balls and the cone does not allow the balls to rotate, so it results in the deterioration of the surface quality [6]. Magnetic chuck table can be applied to repel this phenomenon for the experiments.

After milling [7] and burnishing [8] the surface flatness changes, which has an effect on the operation of the parts. Inappropriate surfaces can cause failures during usage and the evaluation of failure is a complex process, so the capability of the surface quality in the industrial life is especially important [9–11].

2. Magnetic assisted ball burnishing tool

There are many materials in our life, one of them are magnetizable and others are non-magnetizable, both types are important for the industry [12], however, in some cases the original state of the machined workpiece is it not suitable for the required usage. In such certain cases ball burnishing can change the material's roughness, hardness [13,14], corrosion [15] and wearing resistance [16] and decrease the incorporated stress values [17].

* Corresponding author at: Institute for Computer Science and Control, researcher at the John von Neumann Univeristy, Chairperson of the IMEKO TC10 of Testing, Diagnostics & Inspection.
E-mail address: viharos.zsolt@sztaki.hu (Z.J. Viharos).

https://doi.org/10.1016/j.measurement.2020.107750
0263-2241/

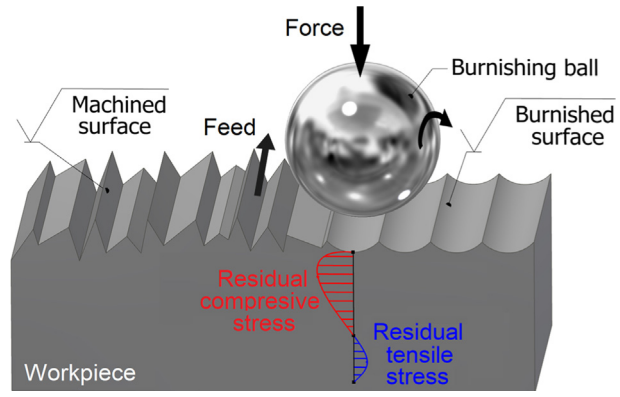

Fig. 1. Principle of ball burnishing.

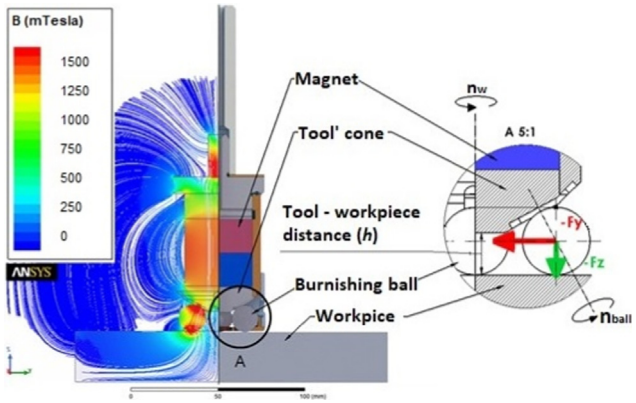

Fig. 2. Parts of MABB tool and the magnetic flux.

In this paper, ball burnishing of various flat materials as C45 steel (1045 steel), X6CrNiTi1811 austenite steel, AA7075 aluminium and PA6 polymer (Polyamide) are investigated. The C45 steel is used as a reference, benchmark material for machining in scientific research and industry [18], so in this study it has also the same role. The X6CrNiTi1811 austenite steel is one of the most commonly used industrial stainless steel [19] and also its machinability is really good. The AA7075 is a highly machinable kind of aluminiums, this the main reason why it has become to the most widely applied aluminium alloy for machining and also it is extensively utilized in aircraft structural parts [20]. The PA6 polymer is used in a wide range of industries [21], it is a typical material for slides, sliding bearings, guide rollers, gears and other machined parts.

2.1. C45 steel

The authors of this paper investigated in their former analysis the effects of ball burnishing on C45 steel applying the novel MABB tool [4]. However, in this preliminary case the main aim was to determine the changes in ferrous materials' hardness and grain size. The C45 is probably the most popular structured steel, so there are several studies in this topic, but cylindrical workpieces were examined in all of them. E.g. Alberto Saldana-Robles at al. have explored that the burnishing force and feed have the main effects on the process (on surface roughness) in case of C45 steel [22].

2.2. Stainless steel

Stainless steels are used in all areas of life, where parts exposed to hard environmental conditions and heavy loads, so it is important to have high strength and corrosion resistance. The burnishing of stainless steels is difficult because of its hardness, so the process requires high burnishing force [23] or special support, like LASER [24]. Lee at al. have studied the ball burnished AISI 316L stainless steel [25], they used a 12 mm ball-ended tool after a milling process for the experiments. They found that the burnishing speed and the type of lubricant affect the surface roughness most significantly, at a 99% level of confidence [25].

2.3. Aluminium

Aluminium and their alloys are widely used by the industry in large quantities because of low density and good mechanical properties [26]. Its burnished surfaces are better according to tribological aspects [27] and harder [28] in case of aluminium, too. As other non-ferrous materials, the aluminium is also burnishable, Adel M. Hassan [29] and M.H. El-Axir et al. [30] explained the effects of ball burnishing of aluminium alloy.

In both studies AA2014 aluminium was applied, both of them burnished a cylindrical workpiece, but Adel M. Hassan manufactured the inner surface while M.H. El-Axir et al. machined the external surface. Their results are very similar, because they stated that the best results for average roughness is obtained when applying high depth of penetration. They reported also that the number of passes depends on both burnishing speed and burnishing feed [30–32].

Also, there are similar studies which evaluated the effect of ball burnishing on aluminium. A.J. Sánchez Egea et al. studied the effect of burnishing strategies on aluminium workpieces which were welded by Friction Stir Welding (FSW) technology [3].

2.4. Plastics

Plastics and plastic-based raw materials play an increasingly important role in the industry [34,35]. Lukasz Janczewski et al. have investigated the burnishing of PE500 polyethylene by diameter of 8 mm ball burnishing tool. Based on their results, the hardness of previously milled polyethylene after burnishing was increased only by 6%, while the wear was decreased by 58% [36]. Fig. 4 reflects their results.

3. Description of the experimental method

The pre-machining process has also a very significant effect before any burnishing [37]. It influences significantly the quality of the burnished's surface (e.g. accuracy and roughness), so analysing their effects is also a very important challenge. Different types of materials require different technological parameters for machining, in the given cases, the workpieces were pre-milled using variations of technological parameters shown in Tables 1–3.

For each workpiece, the feed rates were increased proportionally, indicating that probably the surface roughness values will also increase proportionally.

Because the X6CrNiTi1811 austenite steel, AA7075 aluminium alloy and PA6 polymer are non-magnetizable materials, the necessary burnishing force cannot be generated automatically because

Table 1
Technological parameters for C45.

No.	Feed-v_f (mm/min)	Cutting depth-a_p (mm)	Cutting speed-v_c (m/min)
1	100	1	120
2	200	1	120
3	300	1	120

Table 2
Technological parameters for X6CrNiTi1811.

No.	Feed-v_f (mm/min)	Cutting depth-a_p (mm)	Cutting speed-v_c (m/min)
1	100	1	80
2	200	1	80
3	300	1	80

Table 3
Technological parameters for AA7075 and PA6.

No.	Feed-v_f (mm/min)	Cutting depth-a_p (mm)	Cutting speed-v_c (m/min)
1	500	1	300
2	800	1	300
3	1100	1	300

the magnetic flux circles cannot be formed and closed through the workpiece material. The solution was a magnetic table that was placed under the workpiece, as shown in Fig. 3.

Each specimen was cut to a dimension of 200 × 300 × 12 mm. For the addressed burnishing process experiments the standard Taguchi orthogonal array L9 (3^3) was designed which has three factors and three levels. The experimental results were analysed using the MINITAB 17 software. The created Design of Experiments (DoE) table is shown in Table 4.

The factors in Table 4 are the same, expect the average surface roughness after milling, because there are four pre-milled different materials, as in Table 5.

For the analysis, n = 36 experiments (n = 4 × 9) were carried out, because of the 9 experiments per material, and there were 4 materials available. The pre-milling process produced different Ra roughness, so, it must be handled by the levels of the B factor according to the tested materials, as represented in Table 6.

4. Results and discussions

After the burnishing, using all the designed machining parameters on all the various materials, the surfaces were evaluated by measuring the surface hardness, average surface roughness, and by microscopic pictures were taken about the structure of the modified material layer. The following measuring equipment were used throughout the experimental work: for surface measurement MITUTOYO Formtracer SV-C3000 (uncertainty of the measurement: 0.07 × Ra); Wilson-Wolpert 401 MVD microhardness HV0,1 instrument for Vickers microhardness tests with an optical microscope under a load of 100 g (uncertainty of the measurement: 2–4%); for flatness measurement Mitutoyo Crysta Apex C

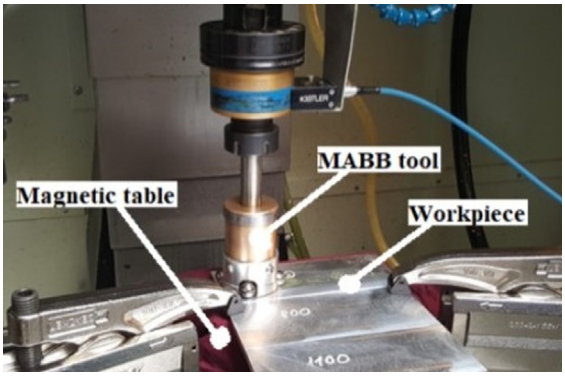

Fig. 3. Designation of experiments.

Table 4
DoE of ball burnishing.

No.	A Feed	B Pre-milled surface roughness	C Burnishing speed
1	1	1	1
2	1	2	2
3	1	3	3
4	2	1	2
5	2	2	3
6	2	3	1
7	3	1	3
8	3	2	1
9	3	3	2

544 3D Coordinate measuring machine (uncertainty of one point measurement: 1.82 μm); for microscopical evaluation a Zeiss Axio Imager.M2m light microscope; and for SEM evaluation a Zeiss EVO MA10 SEM microscope were applied. In the research, the measurement's validations were carried out by based on the instrument's uncertainty.

4.1. Surface roughness

After burnishing, the average surface roughness can be decreased even to 1/10 ratio compared to the original surface. This surface improvement is clearly visible in SEM images, the milled surface in Fig. 4 and the burnished in Fig. 5.

The individual milled and burnished average surface roughness (*Ra*) parameters with the uncertainties of measurement are presented in Fig. 6.

Figs. 7–10 shows three-dimensional fitted curves by a distance based interpolation method, as representation examples for the effects of various combinations of the selected ball burnishing parameters (burnishing speed, feed, pre-milled average surface roughness) on the final Ra roughness of the C45, X6CrNiTi1811, AA7075 and PA6 workpieces after burnishing by the novel MABB tool. It is worth mentioning that each curve represents the effects of two input parameters while the third (burnishing feed-v_f) was kept at that constant level where the resulted roughness was the smallest: in case of C45 and PA6 polymer the v_f = 10 mm/min, while in case of AA7075 and X6CrNiTi1811 the v_f = 30 mm/min produced the lowest average surface roughness.

A surprising result is shown in Fig. 7. (material: C45); if the burnishing speed is high (v_b = 60 m/min) and the pre-milled surface roughness is rough (Ra = 1.105 μm) it provides the lowest final average surface roughness (*Ra* = 0.127 μm) by burnishing, in case of lowest burnishing feed (v_f = 10 mm/min). It means that the burnishing speed has essential effects for the final surface's quality. The suspicion is that the high pre-milling roughness provides relative high amount of material for plastic deformation. Furthermore, the high burnishing speed guarantees the high number of passes on the same material sub-surface.

Fig. 8. (*X6CrNiTi1811 austenite steel*), presents that at low values of the pre-milled surface roughness and burnishing speed, none of these parameters have significant effects on the burnished surface roughness. When the burnishing speed is high the increase of the pre-milled surface roughness results in decrease of the burnishing surface roughness. The effect is reverse in the opposite case, so, at low pre-milled roughness with the burnishing increase of the burnishing speed the burnished surface roughness increases, too.

It is mirrored in Fig. 8. that *the reduction in the burnished surface roughness is caused mainly by the pre-milled surface roughness, indicating that the burnishing speed has less effect for all the examined feed values,* e.g. *in this presented case the burnishing feed has a middle value (v_f = 30 mm/min).*

Table 5
Burnishing factors and levels for the Design of Experiments (DoE).

Factor		Level		
		1	2	3
A	Feed-v_f (mm/min)	10	30	50
B	Pre-milled surface roughness-Ra (μm)	See in the Table 6.		
C	Burnishing speed-v_b (m/min)	20	40	60

Table 6
Average surface roughness (Ra) values after milling, so, before burnishing.

Material	B-1 (μm)	B-2 (μm)	B-3 (μm)
C45	0.672	0.950	1.105
X6CrNiTi1811	1.455	2.553	1.249
AA7075	0.927	1.813	0.873
PA6	1.714	1.628	1.883

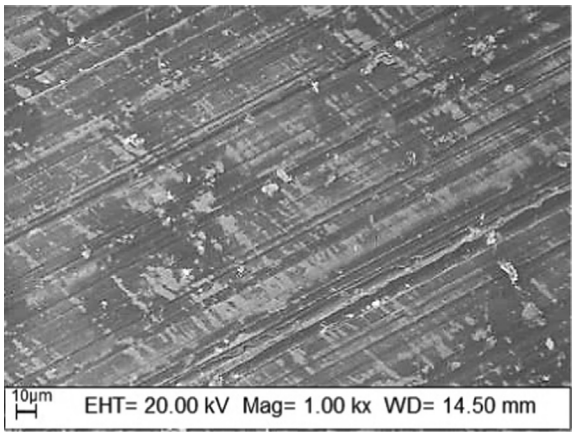

Fig. 4. SEM images of C45 surface after face milling, (v_f = 200 mm/min, v_c = 120 m/min, a_p = 1 mm, *Ra* = 1.105 μm).

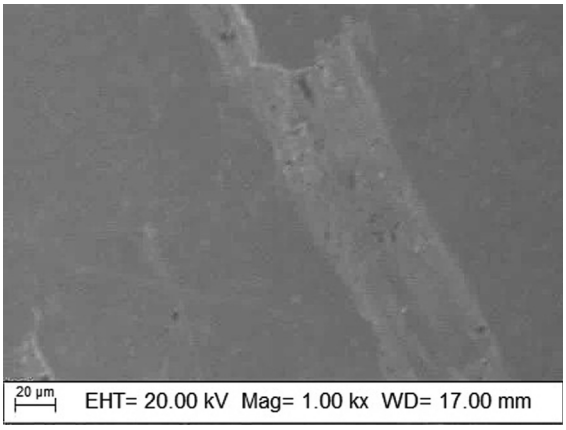

Fig. 5. SEM images of C45 surface after MABB, (v_f = 10 mm/min, v_b = 60 m/min, pre-*Ra* = 1.105 μm, burnished *Ra* = 0.127 μm).

According to Fig. 9. (AA7075 aluminium alloy) it can be concluded that the initial, low roughness of pre-milled surface produces low surface average roughness beside of low burnishing speed. The increase of the burnishing speed increases the surface average roughness, except the high pre-milled surface, because in this case the burnished surface roughness stagnates. This phenomenon is opposite of the experience at C45. The higher burnishing feed (v_f = 30 mm/min) also has positive effect as in the case of X6CrNiTi1811. *The plasticity of AA7075 should be the main reason of this phenomenon.*

In Fig. 10. (*PA6 polymer*) the effects of the machining parameters are similar to the case of C45, so, *the best results were obtained at the highest speed (v_b = 60 m/min) and pre-milling average surface roughness (Ra = 1.761 μm), while the burnishing feed needs to be low (v_f = 10 mm/min), too.*

The search for the optimal conditions for the C45 material were performed, similar, as analysed previously [5], considering the improvement in the burnishing surface roughness through the means of the S/N ratios resulted by the different machining parameters (Fig. 11.).

As shown in Fig. 11, the pre-milled surface roughness (pre. *Ra*) has the most significant effect on the roughness improvement and the determined optimal condition for the highest average roughness improvement is the combination of A3-B1-C3-D3 (v_b: 60 m/min; v_f: 25 mm/min; *h*: 11.5 mm; *Ra*: 1.105 μm).

4.2. Surface hardness

Figs. 12 and 14 show the resulted burnished surface hardness depending on the depth in the material and Figs. 13 and 15 show the microstructure images of C45 after burnishing with the novel MABB tool. The C45 surface material has reached the highest roughness reductions (from Ra = 1.105 μm to Ra = 0.127 μm), consequently, the highest material compaction was realized in this case. At all of the 9 tests the surface hardness of C45 steel get increased up to 220 $HV_{0.1}$ from 185 $HV_{0.1}$ (base material hardness without machining), as represented in Fig. 14.

As the Fig. 12 shows there is a valley in the curve between 0.15 and 0.25 mm depth from the surface, after it, the material hardness reaches the base material hardness. *This phenomena can be discernible at all of the hardness measurements. Because this is rough grain layer was generated between the upper fine grain layer and the grain of the base material (Figs. 13 and 15), so, this transition causes the hardness reduction.*

As the Figs. 12, 14 and 16 show the thickness of the hardening layer is about between 0.2–0.3 mm. This value is more than the author's original expectation, similarly to the values of the hardness. In case of X6CrNiTi1811 and PA6, after the burnishing the compaction of these materials were negligibly small, so it is not possible the evaluation them in this aspect, because of the hardened layer thickness is comparable to the measurement uncertainty range of the $HV_{0.1}$ microhardness measuring instrument. The measured hardness of AA7075 mirrors that the decrease in it was similar to the decrease at C45, as shown in Fig. 16.

The surface hardness of AA7075 get increased up to 200 $HV_{0.1}$ from 165 $HV_{0.1}$ (it is the base material hardness without machining). Figs. 14 and 16 represent that the standard deviations of the measurements are relatively low compared to their measured values. This effect mirrors small uncertainty of the measurements experienced, partly because the measuring instrument has around 2–4% uncertainty according to its specification, consequently the measurements are valid and practically applicable.

5. Evaluation of the surface flatness

According to the ISO 12781-1:2011 standard, the surface flatness tolerance is the linear dimension *a*, which specifies a tolerance zone defined by two parallel planes within which the surface must lie (Fig. 17.) [38].

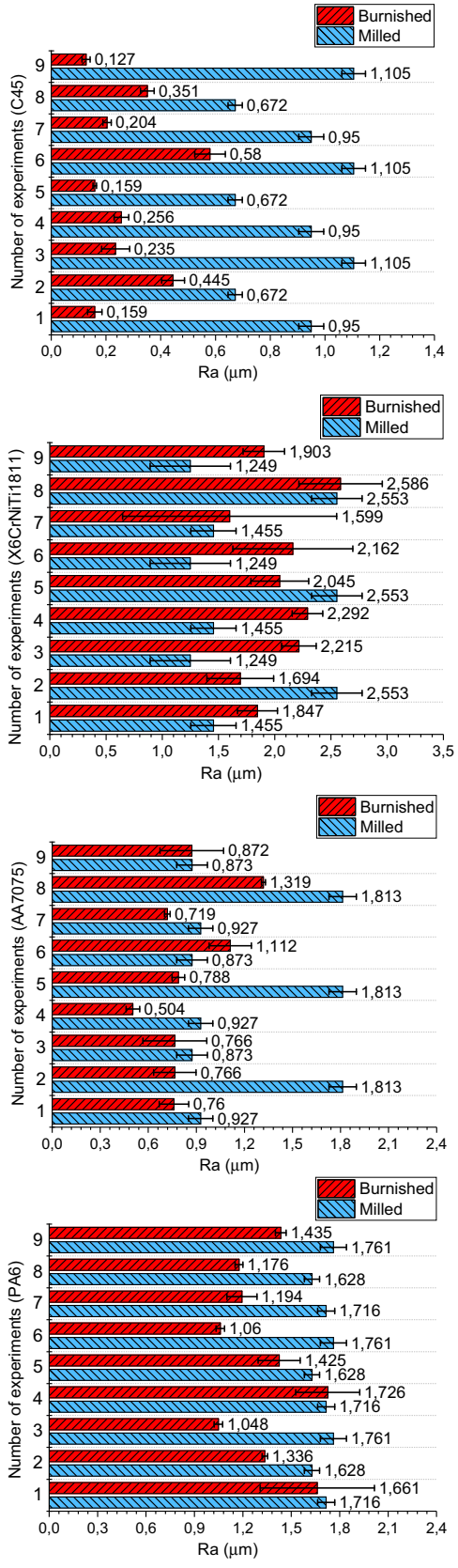

Fig. 6. Average roughness (Ra) parameters after milling and ball burnishing.

Flatness can be measured using a height gauge running across the surface of the part, however, this method requires much patience, training, time and also may contain possible mistakes.

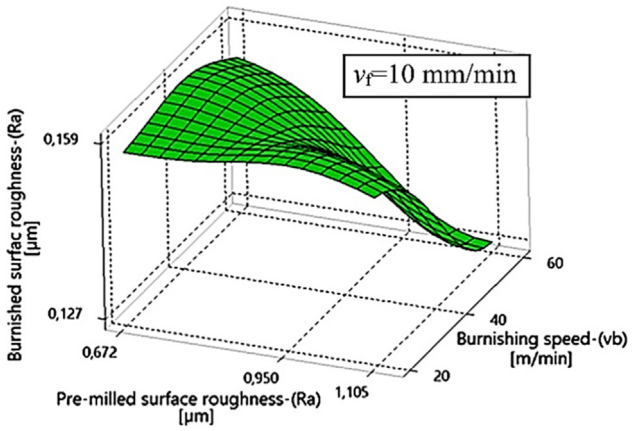

Fig. 7. Effect of burnishing speed and pre-milled surface roughness on surface average roughness of C45.

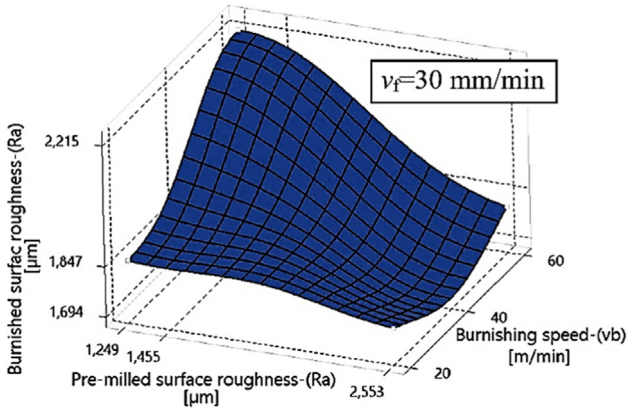

Fig. 8. Effect of burnishing speed and pre-milled surface roughness on surface average roughness of X6CrNiTi1811.

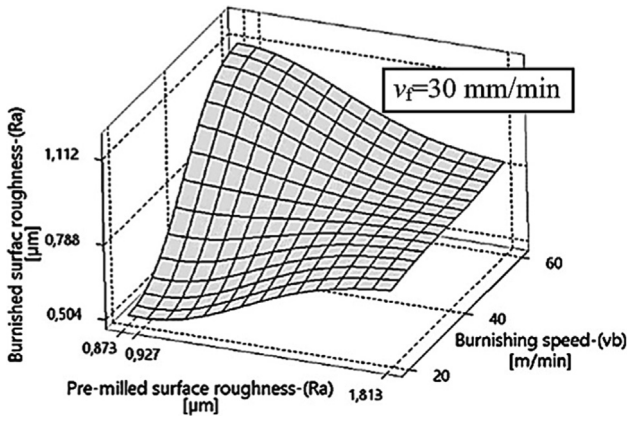

Fig. 9. Effect of burnishing speed and pre-milled surface roughness on surface average roughness of AA7075.

Because the surface of a plane is an area, here, the Coordinate Measuring Machine (CMM) gives an optimal measuring solution and guarantees appropriate results. There are also other alternative measuring systems and methods, like spectral interferometry method [39] or scanning method [40], too.

According to the hardness and roughness results, the surface flatness was evaluated only for the C45 material. The available magnetic table size is the reason for this decision because it does

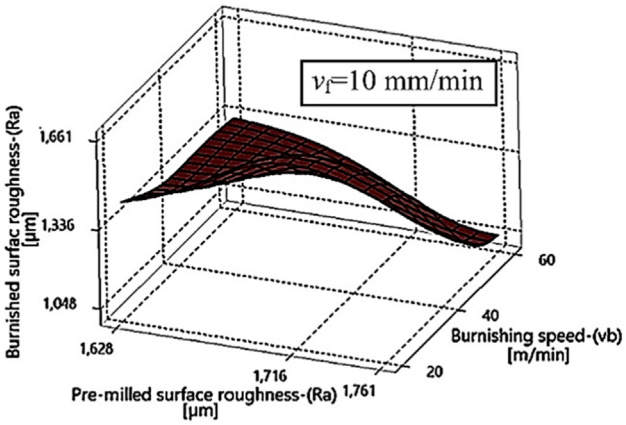

Fig. 10. Effect of burnishing speed and pre-milled surface roughness on surface average roughness of PA6 polymer.

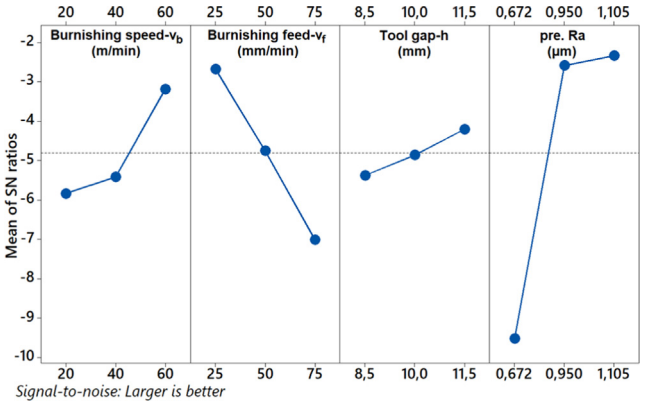

Fig. 11. Effects of the burnishing factors on the surface roughness improvement, in case of C45.

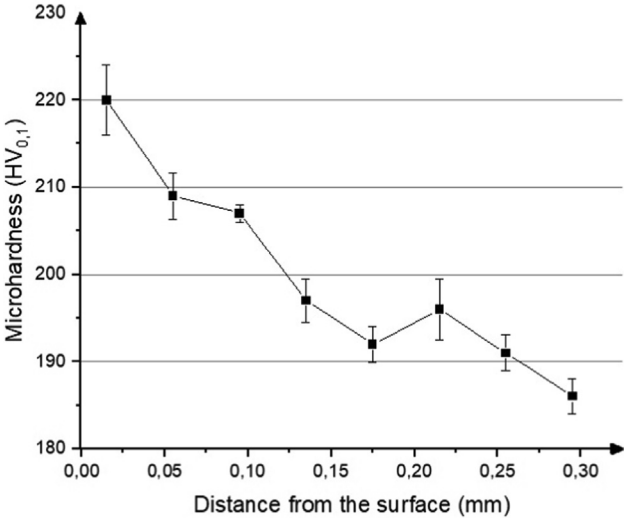

Fig. 12. Surface hardness of and its standard deviation (error bar) C45, No. 5th experiment.

not allow to get a broader burnished surface. The workpieces, presented in a previous research [31] of the authors of this paper, were used for evaluate the flatness, which were burnished by different machining strategies. These strategies allow for MABB technology to get even a wider size of the burnished area.

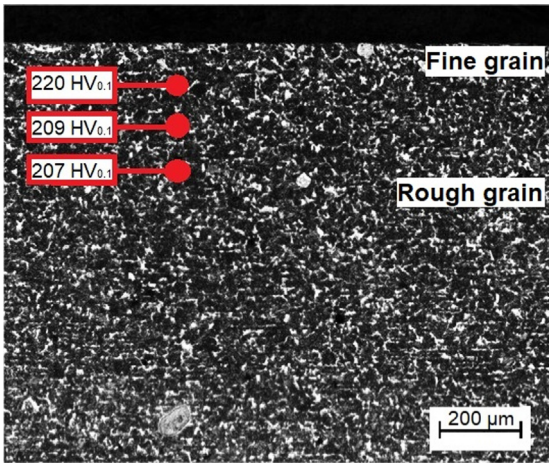

Fig. 13. Microstructure image of C45 surface and the hardness dispersion, No. 5th experiment.

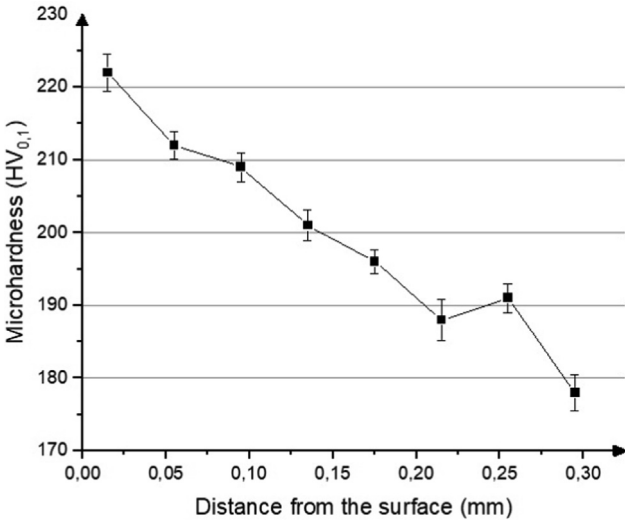

Fig. 14. Surface hardness of C45, No. 6th experiment.

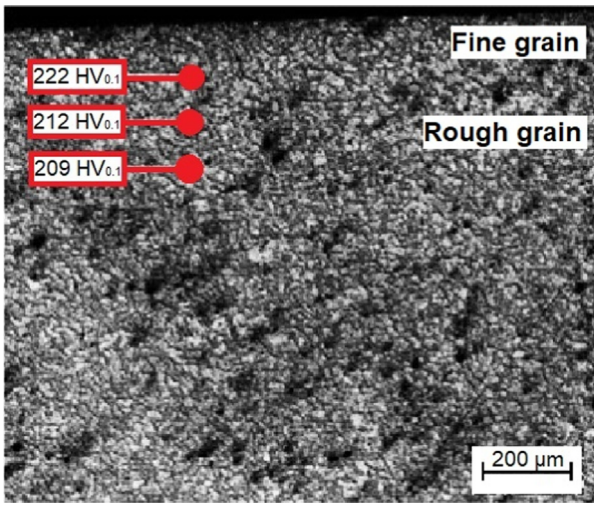

Fig. 15. Microstructure image of C45 surface and the hardness dispersion, No. 6th experiment.

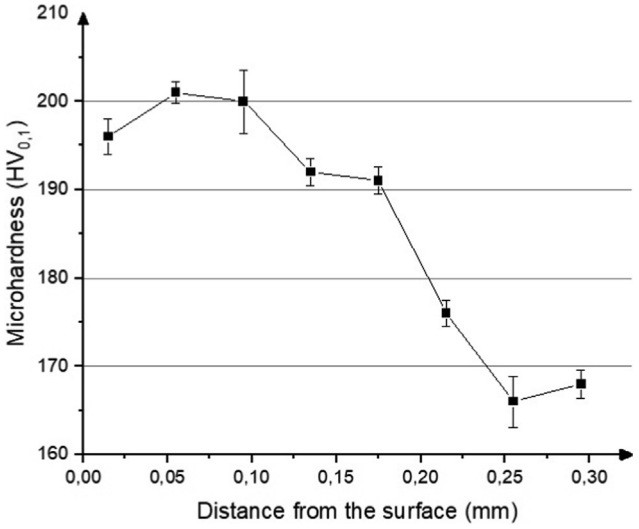

Fig. 16. Surface hardness and its standard deviation (error bar) of AA7075, No. 2nd experiment.

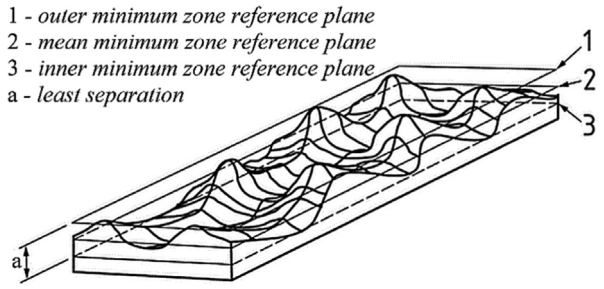

Fig. 17. Minimum zone reference planes (ISO 12781-1:2011) [38].

According to tribological aspects [41], these burnished surfaces are different, so with high probability there are differences among the surface flatness, too. Fig. 18 shows the 5 types of strategies, which were applied for burnishing experiments.

For flatness measurements, the authors used Mitutoyo Crysta Apex C 544 and Renishaw PH10 probe head (Ø3 mm). Before burnishing, the milled surface was measured at 441 points (point distance was constant) on a size of 50 × 50 mm surface by the single point method. This measuring method was applied for all the surfaces. The measurement took about 10 h per sample/surface and the instrument's uncertainty (0.00182 mm) is at least one magnitudes smaller than the measured values (that range is 0.01 mm) indicating that the measurement uncertainty is small enough in this case, too.

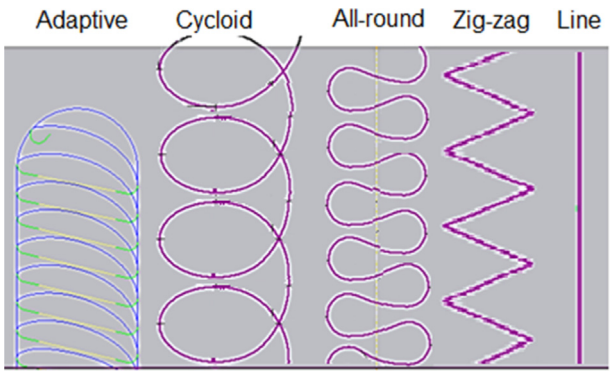

Fig. 18. Ball burnishing strategies.

The measured parameters are presented in Fig. 19 it can be identified that the burnishing has significant effect on the surface flatness, too. Moreover, the surface topologies after milling and burnishing show different forms. The mildest surface flatness error is 0.012 mm, which is better than the burnished surface flatness error. Consequently, it can be concluded that *the burnishing do not improve the surface flatness*, moreover, there are differences among the forms of the surfaces created with different strategies. This phenomena is especially important for the usability of surfaces in the industrial life, e.g. according to tribological aspects, a surface with oil-pockets is beneficial. Thanks for the various burnishing strategies, the number of passes are increasing with the increasing complexity of the strategies in which the paths better overlap each other, so, for those surfaces the value of flatness error is lower. *Consequently, applying the appropriate strategy ensures that the proposed technology can keep the flatness level of the original milled surface*. The Adaptive strategy served with the best results concerning the flatness (macro-geometry), however, the preceding research of the authors proved that the Cycloid strategy improves the average surface roughness (micro-geometry) exceptional significantly, especially in tribological aspects [31]. This diverse effect indicates further research, the cycloid path's loops are promising for ensuring with an optimal, compromise strategy for both the average surface roughness (on micro-level) and flatness (on macro-level), too.

6. Conclusions

The paper reported a comprehensive analysis of surface flatness, roughness and hardness after the proposed magnetic assisted ball burnishing (MABB) of both magnetizable and non-magnetizable workpieces. During the production process, the balls rotate to generate high-speed and long-distance sliding under a constant burnishing force, generated by magnetic flux. Total differently behaving materials were machined (steels, aluminium, polymer) and beyond the analysis of the effects of the varying machining parameters and tool strategies, also the influence of the features of the pre-milling surfaces were examined.

The main conclusions of the paper can be summarized as follows:

- The proposed MABB tool can burnish also non-magnetizable metals and other materials, supported by a magnetic table.
- The best results for average roughness is obtained at low feed rate and if the pre-milled roughness value is large enough for deformation at C45 material.
- At AA7075 aluminium alloy, low average surface roughness can be reached with low technological parameters.
- The machining of X6CrNiTi1811 austenite steel, similarly to AA7075 aluminium alloy, requires low values for the technological parameters.
- The burnishing of PA6 polymer has acceptable roughness reduction, but the process is very sensitive to the technological parameters and other deviations.
- For the highest average roughness improvement on C45, the following technological parameters combination is needed: A3-B1-C3-D3 (v_b: 60 m/min; v_f: 25 mm/min; h: 11.5 mm; Ra: 1.105 μm).
- The hardness of the C45 steel after the proposed MABB machining can be improved by 20%.
- The hardness of the AA7075 aluminium can be improved also by 20%.

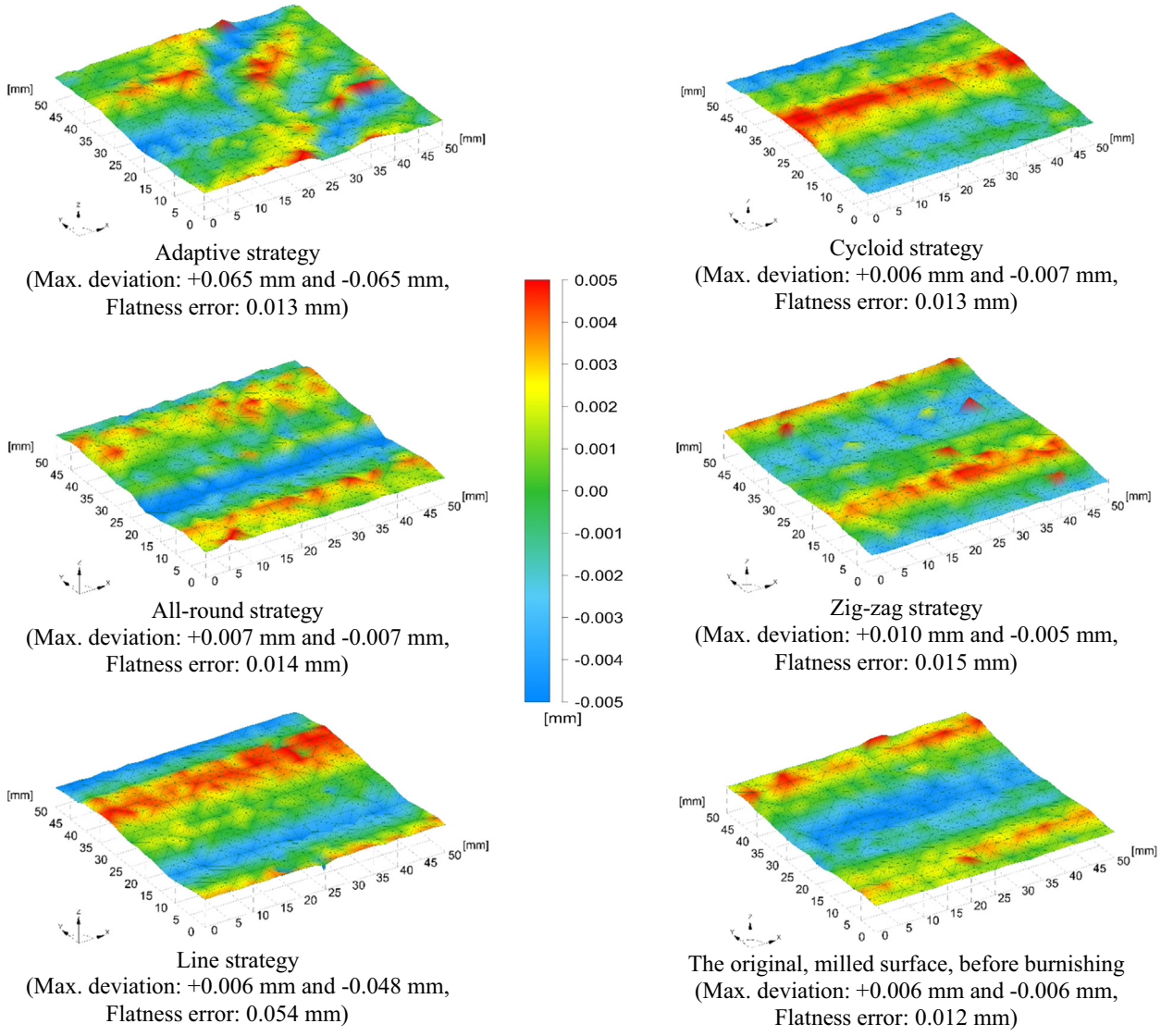

Fig. 19. Surface morphology after milling, and ball burnishing using different strategies.

- The hardened layer thickness reached about between 0.2 and 0.3 mm in case of C45 and A7075 machining.
- The various burnishing strategies can increase and also decrease the flatness error, it is dependent on the number of burnishing passes and strategies.
- The Adaptive strategy served with the best results concerning the flatness; however, the cycloid strategy improves the average surface roughness significantly. This diverse effect indicates further research, the cycloid path's loops are promising for ensuring with an optimal, compromise strategy for both the average surface roughness (on micro-level) and flatness (on macro-level), too.

Results bring forth further research and challenges. The PA6 polymer hardness measurement could not be performed, because the hardness measuring instrument is not suitable for polymer, however, there exists specials hardness measurement instruments designed especially for polymers. In case of X6CrNiTi1811 austenite steel, it is well known that the austenite microstructure is transformed into martensite by mechanical loads, this effect can be analysed, too. Another, short term plan is the measurement of the surface profile macro-geometrical change after burnishing, until now the effects for the surface topological macro-accuracy were not yet explored.

CRediT authorship contribution statement

Zsolt F. Kovács: Conceptualization, Methodology, Software, Validation, Formal analysis, Investigation, Resources, Data curation, Writing - original draft, Writing - review & editing, Visualization, Project administration, Funding acquisition. **Zsolt J. Viharos:** Conceptualization, Methodology, Validation, Formal analysis, Investigation, Resources, Data curation, Writing - original draft, Writing - review & editing, Visualization, Project administration, Funding acquisition. **János Kodácsy:** Conceptualization, Methodology, Validation, Formal analysis, Investigation, Resources, Visualization, Project administration.

Declaration of Competing Interest

The authors declare that they have no known competing financial interests or personal relationships that could have appeared to influence the work reported in this paper.

Acknowledgements

This research is party supported by EFOP-3.6.1-16-2016-00006 "The development and enhancement of the research potential at John von Neumann University" project. The Project is supported by the Hungarian Government and co-financed by the European Social Fund.

The research reported in this paper was supported by the Higher Education Excellence Program of the Ministry of Human Capacities in the frame of Nanotechnology research area of Budapest University of Technology and Economics (BME FIKP-NANO).

The research in this paper was (partially) supported by the European Commission through the H2020 project EPIC (https://www.centre-epic.eu/) under grant No. 739592 and by the Hungarian ED_18-2-2018-0006 grant on an "Research on prime exploitation of the potential provided by the industrial digitalisation".

References

[1] János Kundrák, Vladimir Fedorovich, Ivan Pyzhov, Angelos P. Markopoulos, Improving the effectiveness of combined grinding processes for processing superhard materials, J. Manuf. Processes 43 (2019) 270–275.
[2] J. Kundrák, V. Fedorovich, A.P. Markopoulos, I. Pyzhov, N. Kryukova, Diamond grinding wheels production study with the use of the finite element method, J. Adv. Res. (2016) 1057–1064.
[3] A.J. Sánchez Egea, A. Rodríguez, D. Celentano, A. Calleja, L.N. López de Lacalle: Joining metrics enhancement when combining FSW and ball-burnishing in a 2050 aluminium alloy, Surface & Coatings Technology 367 (2019), pp. 327–335.
[4] Zs. F. Kovács, Zs. J. Viharos, J. Kodácsy: Making twist-free surfaces by magnetic assisted ball burnishing, Solid State Phenomena 261 (2017) 159–166.
[5] Zs. F. Kovács, Zs. J. Viharos, J. Kodácsy: Determination of the working gap and optimal machining parameters for magnetic assisted ball burnishing, Measurement 118 (2018) 172–180.
[6] Zs. F. Kovács, Zs. J. Viharos, J. Kodácsy: Determination of the optimal working gap for the magnetic assisted ball burnishing tool, International Measurement Confederation (IMEKO) (2017) 170–175.
[7] Saurin Sheth, P M george: experimental investigation and prediction of flatness and surface roughness during face milling operation of WCB material, Procedia Technol. 23 (2016) 344–351.
[8] R. Jerez-Mesa, Y. Landon, J.A. Travieso-Rodriguez, G. Dessein, J. Lluma-Fuentes, V. Wagner, Topological surface integrity modification of AISI 1038 alloy after vibrationassisted ball burnishing, Surf. Coat. Technol. 349 (2018) 364–377.
[9] Lorenzo Ciani, Giulia Guidi, Application and analysis of methods for the evaluation of failure rate distribution parameters for avionics components, Measurement 139 (2019) 258–269.
[10] Vladimir V. Sinitsin, Roller bearing fault detection by applying wireless sensor of instantaneous accelerations of mechanisms moving elements, International Measurement Confederation (IMEKO) (2017) 62–66.
[11] O. Niculita, Design and development of a testbed capable of supporting technical diagnostics of complex systems, Journal of Physics: Conf. Series 1065 (2018) 102019.
[12] Saverio Affatato, Massimiliano Merola, Alessandro Ruggiero, Tribological performances of total knee prostheses: roughness measurements on medial and lateral compartments of retrieved femoral components, Measurement 135 (2019) 341–347.
[13] Alberto Saldaña-Robles, Héctor Plascencia-Mora, Eduardo Aguilera-Gómez, Adriana Saldaña-Robles, Alfredo Marquez-Herrera, José Angel Diosdado-De la Peña: Influence of ball-burnishing on roughness, hardness and corrosion resistance of AISI 1045 steel, Surface Coatings Technol 339 (2018) 191–198.
[14] Goutam D. Revankar, Raviraj Shetty, Shrikantha S. Rao, Vinayak N. Gaitonde, Analysis of surface roughness and hardness in ball burnishing of titanium alloy, Measurement 58 (2014) 256–268.
[15] Kazimiera Konefal, Mieczyslaw Korzynski, Zofia Byczkowska, Katarzyna Korzynska, Improved corrosion resistance of stainless steel X6CrNiMoTi17-12-2by slide diamond burnishing, J. Mater. Process. Technol. 213 (2013) 1997–2004.
[16] Goutam Devaraya Revankar, Raviraj Shetty, Shrikantha Srinivas Rao, Vinayak Neelakanth Gaitonde, Wear resistance enhancement of titanium alloy (Ti–6Al–4V) by ball burnishing process, J. Mater. Res. Technol. 6 (2017) 13–32.
[17] Reza Teimouri, Saeid Amini, Alireza Bagheri Bami, Evaluation of optimized surface properties and residual stress in ultrasonic assisted ball burnishing of AA6061-T6, Measurement 116 (2018) 129–139.
[18] Tadeusz Leppert, Effect of cooling and lubrication conditions on surface topography and turning process of C45 steel, Int. J. Mach. Tools Manuf 51 (2011) 120–126.
[19] M. Grosse, M. Niffenegger, D. Kalkhof, Monitoring of low-cycle fatigue degradation in X6CrNiTi18-10 austenitic steel, J. Nucl. Mater. 296 (2001) 305–311.
[20] P. Rambabu, N. Eswara Prasad, V.V. Kutumbarao, R.J.H. Wanhill, Aluminium alloys for aerospace applications, Aerospace Materials and Material Technologies, 2016, p. 29–52.
[21] Zizhen Wei, Rui Wang, Jianfeng Wang, Yanyu Yang, Yukun Liu, Wanjie Wang, Yanxia Cao, Highly toughened PA6 using residue of plasticized PVB film via two-step reactive melt blending, Polymer 186 (2020) 122052.
[22] A. Saldaña-Roblesa, H. Plascencia-Morab, E. Aguilera-Gómezb, A. Saldaña-Roblesa, A. Marquez-Herreraa, J.A. Diosdado-De la Peña, Influence of ball-burnishing on roughness, hardness and corrosion resistance of AISI 1045 steel, Surf. Coat. Technol. 339 (2018) 191–198.
[23] S. Ś wirad, D. Wydrzynski, P. Nieslony, G.M. Krolczy.k: Influence of hydrostatic burnishing strategy on the surface topography of martensitic steel, Measurement 138 (2019) 590–601.
[24] C. Courbon, A. Sova, F. Valiorgue, H. Pascal, J. Sijobert, G. Kermouche, Ph. Bertrand, J. Rech, Near surface transformations of stainless steel cold spray and laser cladding deposits after turning and ball-burnishing, Surf. Coat. Technol. 371 (2019) 235–244.
[25] S.S.G. Lee, S.C. Tam, N.H. Loh, Ball burnishing of 316L stainless steel, J. Mater. Process. Technol. 37 (1993) 241–251.
[26] Hasan Yilmaz, Recep Sadeler, Impact wear behavior of ball burnished 316L stainless steel, Surf. Coat. Technol. 363 (2019) 369–378.
[27] N.S.M. El-Tayeb, K.O. Low, P.V. Brevern, Influence of roller burnishing contact width and burnishing orientation on surface quality and tribological behaviour of Aluminium 6061, J. Mater. Process. Technol. 186 (2007) 272–278.
[28] V. Jaya Prasad, K. Sam Joshi, V.S.N. Venkata Ramana, R. Chiranjeevi. Effect of roller burnishing on surface properties of wrought AA6063 aluminium alloys, Materials Today: Proceedings 5 (2018) 8033–8040.
[29] A.M. Hassan, The effects of ball- and roller-burnishing on the surface roughness and hardness of some non-ferrous metals, J. Mater. Process. Technol. 72 (1997) 385–391.
[30] M.H. El-Axir, O.M. Othmanb, A.M. Abodiena, Study on the inner surface finishing of aluminum alloy 2014 by ball burnishing process, Journal of Materials Processing Technology 202 (2008) 435–442.
[31] Zs. F. Kovács, Zs. J. Viharos, J. Kodácsy, The effects of machining strategies of magnetic assisted roller burnishing on the resulted surface structure, Mater. Sci. Eng. 448 (2018) 1–8.
[32] S.R. Thorat, A.G. Thakur, Optimization of burnishing parameters by taguchi based GRA method of AA 6061 aluminum alloy, Mater. Today. Proc. 5 (2018) 7394–7403.
[34] Norbert Geier, J. Paulo Davim, Tibor Szalay, Advanced cutting tools and technologies for drilling carbon fibre reinforced polymer (CFRP) composites: a review, Compos. A Appl. Sci. Manuf. 125 (2019) 105552.
[35] Norbert Geier, Tibor Szalay, Márton Takács, Analysis of thrust force and characteristics of uncut fibres at non-conventional oriented drilling of unidirectional carbon fibre-reinforced plastic (UD-CFRP) composite laminates, Int. J. Adv. Manufact. Technol. 100 (9–12) (2019) 3139–3154.
[36] Ł. Janczewski, D. Toboła, W. Brostow, K. Czechowski, H.E.H. Lobland, M. Kot, K. Zagórski, Effects of ball burnishing on surface properties of low density polyethylene, Tribol. Int. 93 (2019) 36–42.
[37] István Biró, Miklós Czampa1, Tibor Szalay, Experimental model for the main cutting force in face milling of a high strength structural steel, Periodica Polytechnica Mechanical Engineering 59 (1) (2015) 16–22.
[38] Geometrical product specifications (GPS). Flatness. Part 1: Vocabulary and parameters of flatness (ISO 12781-1:2011).
[39] H.C. Kandpal, Ranjana Mehrotra, Swati Raman, Determination of surface flatness by spectral interferometric method, Opt. Lasers Eng. 43 (2005) 1315–1321.
[40] Jerzy Sładek, Paweł M. Błaszczyk, Magdalena Kupiec, Robert Sitnik, The hybrid contact–optical coordinate measuring system, Measurement 44 (2011) 503–510.
[41] Jan Liska, Zdenko Lipa, Ivan Baranek, Katarina Siketova: Superfinishing theory, Annals of DAAAM for 2009 & Proceedings of the 20th International DAAAM Symposium (2009) 1297–1298.